

Early results from GLASS-JWST XVI: Discovering a bluer $z \sim 4 - 7$ Universe through UV slopes

THEMIYA NANAYAKKARA,¹ KARL GLAZEBROOK,¹ COLIN JACOBS,¹ ANDREA BONCHI,² MARCO CASTELLANO,³
ADRIANO FONTANA,³ CHARLOTTE MASON,^{4,5} EMILIANO MERLIN,³ TAKAHIRO MORISHITA,⁶ DIEGO PARIS,³ MICHELE TRENTI,^{7,8}
TOMMASO TREU,⁹ ANTONELLO CALABRÒ,¹⁰ KRISTAN BOYETT,^{7,8} MARUSA BRADAC,^{11,12} NICHIA LEETHOCHAWALIT,^{7,8,13}
DANILO MARCHESINI,¹⁴ PAOLA SANTINI,¹⁰ VICTORIA STRAIT,^{15,16} EROS VANZELLA,¹⁷ BENEDETTA VULCANI,¹⁸ XIN WANG,¹⁹ AND
LILIAN YANG²⁰

¹Centre for Astrophysics and Supercomputing, Swinburne University of Technology, PO Box 218, Hawthorn, VIC 3122, Australia

²Space Science Data Center, Italian Space Agency, via del Politecnico, 00133, Roma, Italy

³INAF - Osservatorio Astronomico di Roma, via di Frascati 33, 00078 Monte Porzio Catone, Italy

⁴Cosmic Dawn Center (DAWN)

⁵Niels Bohr Institute, University of Copenhagen, Jagtvej 128, 2200 København N, Denmark

⁶IPAC, California Institute of Technology, MC 314-6, 1200 E. California Boulevard, Pasadena, CA 91125, USA

⁷School of Physics, University of Melbourne, Parkville 3010, VIC, Australia

⁸ARC Centre of Excellence for All Sky Astrophysics in 3 Dimensions (ASTRO 3D), Australia

⁹Department of Physics and Astronomy, University of California, Los Angeles, 430 Portola Plaza, Los Angeles, CA 90095, USA

¹⁰INAF Osservatorio Astronomico di Roma, Via di Frascati 33, 00078 Monte Porzio Catone, Rome, Italy

¹¹University of Ljubljana, Department of Mathematics and Physics, Jadranska ulica 19, SI-1000 Ljubljana, Slovenia

¹²Department of Physics and Astronomy, University of California Davis, 1 Shields Avenue, Davis, CA 95616, USA

¹³National Astronomical Research Institute of Thailand (NARIT), Mae Rim, Chiang Mai, 50180, Thailand

¹⁴Department of Physics and Astronomy, Tufts University, 574 Boston Ave., Medford, MA 02155, USA

¹⁵Cosmic Dawn Center (DAWN), Denmark

¹⁶Niels Bohr Institute, University of Copenhagen, Jagtvej 128, DK-2200 Copenhagen N, Denmark

¹⁷INAF – OAS, Osservatorio di Astrofisica e Scienza dello Spazio di Bologna, via Gobetti 93/3, I-40129 Bologna, Italy

¹⁸INAF Osservatorio Astronomico di Padova, vicolo dell'Osservatorio 5, 35122 Padova, Italy

¹⁹Infrared Processing and Analysis Center, Caltech, 1200 E. California Blvd., Pasadena, CA 91125, USA

²⁰Kavli Institute for the Physics and Mathematics of the Universe, The University of Tokyo, Kashiwa, Japan 277-8583

Submitted to ApJL

ABSTRACT

We use the JWST-GLASS Early Release Science NIRC*am* parallel observations to provide a first view of the UV continuum properties of NIRC*am*/*F444W* selected galaxies at $4 < z < 7$. We expect the $5\mu\text{m}$ selection to have greater sensitivity to redder systems compared to previous *HST* observations. By combining multi wavelength NIRC*am* observations, we constrain the UV continuum slope for a sample of 178 galaxies with stringent quality controls. Contrary to our expectation, we find that $> 95\%$ of the galaxies are blue star-forming galaxies with very low levels of dust ($A_{v\beta} \sim 0.06 \pm 0.39$). Galaxies with $M_{\text{UV}} < -20$ show evidence for a statistically significant correlation between UV slope and redshift. Fainter and lower mass galaxies show bluer UV slopes compared to their brighter high mass counterparts. Individual fits to galaxies reach the bluest UV slope values of $\beta \sim -2.5$ allowed by traditional stellar population models. Therefore, it is likely that stellar population models with Population III contributions or other exotic effects that are not considered currently are required to accurately reproduce the rest-UV and optical observations of galaxies obtained by GLASS-JWST. This dust free early view confirms that our current cosmological understanding of gradual mass + dust buildup of galaxies with cosmic time is largely accurate to describe the $\sim 0.7 - 1.5$ Gyr age window of the Universe. The abundance of a large population of UV faint dust poor systems may point to a dominance of low mass galaxies at $z > 6$ playing a vital role in cosmic reionization.

1. INTRODUCTION

In the current cosmological picture we expect the first galaxies to emerge $\sim 200 - 300$ Myrs after the Big Bang (e.g. Bromm & Yoshida 2011). These galaxies would rapidly build up their stellar masses driving the chemical evolution-

ary processes of the Universe (e.g. Madau & Dickinson 2014; Dayal & Ferrara 2018). Dust/metals produced as end products of stellar evolution in the early galaxies provide key constraints to how cosmic star-formation would have evolved in the first ~ 3 billion years of the Universe (e.g. Stark 2016).

Thus, establishing a relationship between dust and luminosity in the early Universe from UV bright to faint galaxies would provide tight constraints to galaxy evolution and cosmology (e.g. Naidu et al. 2019; Bouwens et al. 2021, 2022b; Finkelstein et al. 2022; Leethochawalit et al. 2022; Le Reste et al. 2022).

Previous *Hubble Space Telescope* (*HST*) and *Spitzer* observations have been able to detect galaxies in the early Universe shedding light on early cosmic processes (see Bradač (2020) for a review, also Stefanon et al. (2021); Strait et al. (2021); Bouwens et al. (2022a); Finkelstein et al. (2022)). However, these observations have limitations that hinder their diagnostic power in the early Universe. For example, *HST* observations probe the rest frame UV which may be biased towards young stellar populations unobscured by dust while *Spitzer* can only provide constraints on emission lines or strong spectral features like Balmer breaks (e.g. Stefanon et al. 2022).

Spectroscopic observations of high- z sources with Ly- α provide additional galaxy constraints on gas and dust geometries (e.g. Oesch et al. 2015; Matthee et al. 2018; Jung et al. 2019), albeit with limitations (Leonova et al. 2021; Endsley & Stark 2022). ALMA has been successful in detecting large numbers of sources at $z > 6$ in dust emission with high-efficiency (e.g. Hashimoto et al. 2018; Bouwens et al. 2022c), but galaxy selections for ALMA followup are strongly biased towards UV bright sources (e.g. Bouwens et al. 2022c). Thus, even with recent advancements, the formation timescales of galaxies in the early Universe and their UV luminosity, mass, and dust evolution are not well constrained (Dayal et al. 2022; Finkelstein et al. 2022; Tacchella et al. 2022).

The launch of the *James Webb Space Telescope* opened up a new window for exploring galaxy evolution in the early Universe. With JWST/NIRCam NIR $5\mu\text{m}$ selection (*F444W*), JWST can obtain a diverse sample of galaxies in rest-frame optical wavelengths (e.g. Yang et al. (Paper V, submitted), Jacobs et al. (Paper XIV, in. prep)) at $z \sim 4 - 7$. In this analysis we use JWST NIRCam (Burriesci 2005) parallel observations from the GLASS-JWST survey (Treu et al. 2022) to explore the relationship between UV magnitude and UV slope for galaxies between $z \sim 4 - 7$.

The rest-UV slope is a common indicator for dust attenuation and has been used to explore the buildup of dust in the $z \sim 2 - 10$ Universe (e.g. Reddy et al. 2018). While the UV slope could also be degenerate with metallicity and star-formation history (SFH, e.g. Bouwens et al. 2016b), at fixed UV luminosity galaxies with redder UV slopes have been shown to be dustier compared to their bluer counterparts (Reddy et al. 2018). Additionally, at lower metallicities the indications are that galaxies prefer steeper attenuation curves (Reddy et al. 2018). This means that sight lines of young blue stars in low metallicity galaxies have more dust.

While significant evidence for dust has been hinted by recent ALMA detections, the UV slope evolution between $z \sim 4 - 10$ with UV luminosity is still unclear (e.g. Wilkins et al. 2016; Roberts-Borsani et al. 2022). Studies of UV fainter galaxies are largely from *Hubble* frontier fields, boosted by

lensing magnifications (e.g. Yang et al. 2022), but limited to small volumes. At brighter magnitudes, comparisons between field and cluster (lensed) sample UV slopes are found to be largely consistent (Bouwens et al. 2021, 2022b; Yang et al. 2022), there are no independent (non lensed) constraints to the faint end of the UV luminosity function.

With GLASS-JWST rest-frame optical selection we can constrain the UV slopes of UV faint/red galaxies to investigate whether galaxies are faint due to presence of large amounts of intervening dust or whether they are intrinsically faint in UV due to low star-formation. The presence of UV faint high mass galaxies with shallow UV slopes could lead to significant implications to mass buildup of galaxies at $z > 4$.

In Section 2, we describe our sample selection and UV slope calculation process. In Section 3, we interpret our observations in terms of UV luminosity and dust buildup in the early Universe. Finally, in Section 4 provide a summary of our results and discuss how future surveys would provide tighter constraints to the our cosmological understanding. Unless otherwise stated, we assume a Chabrier (2003) IMF and a cosmology with $H_0 = 70 \text{ km/s/Mpc}$, $\Omega_\Lambda = 0.7$ and $\Omega_m = 0.3$. All magnitudes are expressed using the AB system (Oke & Gunn 1983).

2. SAMPLE SELECTION AND UV SLOPE MEASUREMENTS

Our sample is based on the JWST GLASS Early Release Science Program Parallel NIRCam observations (Merlin et al. submitted, henceforth Paper II). The observations used here were obtained on 28-29th of June 2022 as one of the two equal depth observations planned for JWST GLASS using NIRCam filters *F090W*, *F115W*, *F150W*, *F200W*, *F277W*, *F356W*, *F444W*. The *F444W* band was selected for source detection and all images were PSF matched to this band producing a catalogue reaching typical $5\text{-}\sigma$ depths of $\sim 29.0 - 29.7$ mags in all bands. More details on the observations, data reduction, and catalogue generation can be found in Paper II.

For the analysis presented in this paper, we required the selected sample to be covered in both rest-frame UV and optical wavelengths in the 7 JWST/NIRCam bands. The rest-frame UV coverage allows us to investigate the accuracy of the best fit SED shape with the observed photometry. The rest-frame optical coverage includes the balmer break and strong emission lines such as $H\alpha$ and $[\text{O III}]\lambda 5007$. Therefore, our final redshift selection for this work is between $4 < z < 7$. Figure 1 show the observed band coverage for galaxies in this redshift window.

We ran the photometric redshift fitting code EAZY (Brammer et al. 2008) using the eazy-py python wrapper¹ to derive photometric redshifts and rest-frame colors for the Paper II catalogue. We used the eazy_v1.3.spectra.param templates provided by EAZY and the total flux measured in 3FWHM PSF matched NIRCam image apertures. Out of

¹ <https://eazy-py.readthedocs.io>

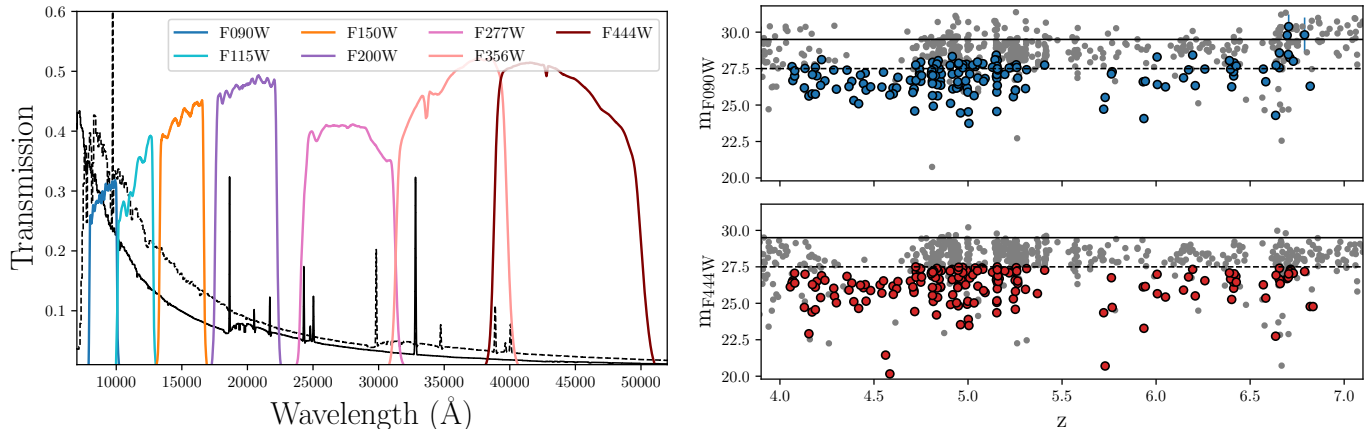


Figure 1. Left: The NIRCam filter coverage of the JWST GLASS Early Release Science Program observations. In total, observations are obtained over seven NIR filters reaching a $5\text{-}\sigma$ depth of $m \sim 29.0 - 29.5$. We also show an example EAzy template of a galaxy at $z = 4.0$ (solid lines) and $z = 7.0$ (dashed lines), the lower and upper z limits used in our sample selection. With this selection, all our galaxies have rest-frame UV and optical coverage which enables stronger constraints to the overall shape of the SED. **Right:** Photometric properties of the sample used in our analysis. We show the magnitude vs redshift distribution of our galaxies in the bluest (**Top:** $F090W$) and reddest (**Bottom:** $F444W$) bands observed by our survey. The grey dots are the galaxies removed from our analysis based on the stringent quality cuts outlined in Section 2. The horizontal solid line is the nominal $5\text{-}\sigma$ detection level of $m = 29.5$ for GLASS_ERS. The horizontal dashed line is the $F444W$ $m < 27.5$ selection limit imposed on the data. The typical error bars for most galaxies are smaller than the marker size.

6590 objects in the catalogue, 731 objects were selected in the redshift window of interest. We then applied a magnitude cut at $F444W < 27.5$ (rest-frame $\sim 5000 - 10000\text{\AA}$), resulting in 270 magnitude limited galaxies. We further pruned this sample by applying stringent quality cuts as follows. First we required galaxies to be detected with a signal to noise (S/N) > 5 in at least 4 photometric bands. This resulted in a sample of 208 galaxies which were detected in a majority of the GLASS-JWST filters. We then visually inspected all the EAzy fit SEDs of the galaxies to determine that there were no failed fits. We defined a fit as a fail if a majority of the observed photometric data points did not agree with the template derived flux within photometric errors, i.e. $1\text{-}\sigma$ outliers. We further visually inspected images of the galaxies in the 7 GLASS-JWST filters and removed sources that were spurious, i.e. sources at the edges of the detectors, sources contaminated with bright neighbors, fragments of stellar spikes, misidentified stars (see Paper II for details). These stringent cuts resulted in a 178 galaxies with high quality photometry and SED fits. Most galaxies that are removed from the sample lie on the redshift range with the highest number of detections ($z \sim 4.5 - 5.5$).

The magnitude distribution of our final sample in the bluest ($F090W$) and reddest ($F444W$) filters as a function of redshift is shown by Figure 1. The majority of our galaxies lie in the $4.5 \lesssim z \lesssim 5.5$ window. Galaxies span a wider range in magnitude in the redder $F444W$ filter ($m_{\text{median}} = 26.5 \pm 1.2$) compared to the bluer $F090W$ filter ($m_{\text{median}} = 27.0 \pm 1.0$). However, galaxies are on average 0.5 mag redder in the blue filters. We find that most galaxies removed by our quality cuts are generally $F444W$ faint galaxies.

We present the EAzy derived rest-frame colors of our sample in Figure 2. This rest-frame $U - V$ vs $V - J$ color space has been shown to be effective in distinguishing between quiescent and star-forming galaxies with high efficiency (Williams et al. 2009; Schreiber et al. 2018b). Based on our photometric redshifts, most of the galaxies in our sample fall in the blue star-forming region of the UVJ color space. Although the purity of quiescent galaxies from this UVJ diagram is high (Schreiber et al. 2018b), studies have shown that galaxies that abruptly quench the star-formation can be excluded from being identified as quiescent in this diagram (e.g., Merlin et al. 2019).

In Figure 2 we further show the $u_s - g_s$ vs $g_s - i_s$ color distribution of our sample to investigate whether we are missing quiescent galaxies that could be missed by the traditional UVJ color selection (Antwi-Danso et al. 2022). We find the classification between star-forming and quiescent to be largely consistent between the two selection methods and that our sample almost exclusively contain blue star-forming systems (quiescent and dusty star-forming galaxies comprise $\lesssim 5\%$ of the total sample). We find a similar result even if we remove the $F444W$ magnitude cut from our sample selection. However, we note that the shape of rest-UVJ selected quiescent galaxy SEDs are similar to that of star-forming galaxies. This is likely driven by the contamination of the rest- V band by strong emission lines at $5 < z < 6$. We defer the full analysis of UVJ selection at $z > 5$ for future work and consider the $> 95\%$ fraction of star-forming galaxies as a lower limit.

We use the best-fit EAzy SEDs to compute the UV slope and UV magnitude of our sample similar to the process outlined by Nanayakkara et al. (2020). We first define a box

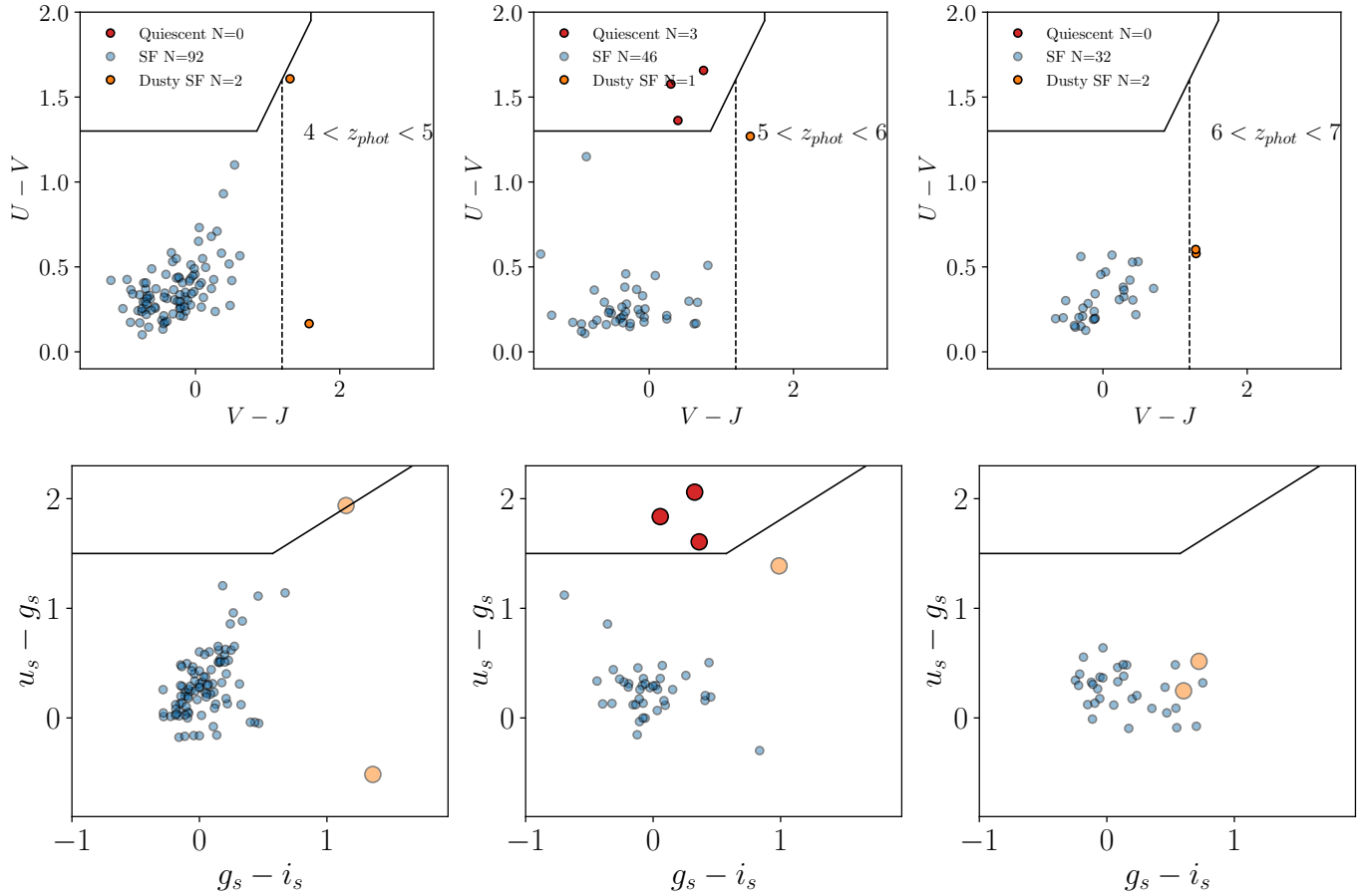


Figure 2. Understanding the rest-frame color distribution of our sample. **Top:** The Rest-frame $U - V$ vs $V - J$ (UVJ) and **Bottom:** $u_s - g_s$ vs $g_s - i_s$ (ugi) color distribution of our sample. We divide the sample into three redshift bins as annotated in the figures. Galaxies are colour coded as blue star-forming (blue circles), red/dusty star-forming (orange circles), and quiescent (red circles) following the selection criteria outlined by Spitler et al. (2014) in UVJ color space. Galaxies classified in UVJ space are shown by similar colors in the ugi color space. The size of red/dusty star-forming and quiescent markers are increased for clarity. Majority of galaxies ($> 95\%$) are categorized as (blue) star-forming in both techniques.

car filter between $\Delta\lambda = 1400 - 2000\text{\AA}$ and compute the UV magnitude from the EAZY best-fit SEDs. Next, for each SED we select a wavelength window between $\Delta\lambda = 1400 - 2000\text{\AA}$ and mask out emission line regions within this window following masks outlined by Calzetti et al. (1994). We then use the masked SEDs to compute the UV continuum slope β by fitting a power-law function using `lmfit` (Newville et al. 2014). We found a single power law to be an accurate description to the UV slopes of all the galaxies in our sample. Figure 3 shows EAZY best-fit SEDs of a representative sample of galaxies presented in our analysis.

We compute stellar masses for our sample using `fast++` (Schreiber et al. 2018b) at the EAZY best-fit redshift. We use Bruzual & Charlot (2003) stellar population models with a Chabrier (2003) IMF, a truncated SFH with a constant and an exponentially declining SFH component, and a Calzetti et al. (2000) dust law.

In Figure 4, we show the relationship of the UV continuum slope with redshift, UV magnitude, and stellar mass.

In Table 1 we tabulate the binned values observed for these three relationships. The UV slope of galaxies does not show any statistically significant correlation with redshift. The $4.5 < z < 5.5$ redshift window with the largest amount of galaxies shows the lowest β values. At later times a gradual flattening of UV slopes is observed.

The UV magnitudes of our sample peaks at $M_{UV} \sim -19$. We observe a slight negative correlation between UV continuum slope and UV magnitude for our binned values. However, individual galaxies do not show statistically significant correlation as parameterized by the Spearman correlation coefficient (Spearman 1904). Some galaxies at $M_{UV} < -21$ reach a clear minimum for UV slopes. This may suggest a limitation on the input SED templates not being able to produce UV slopes blueward of $\lesssim -2.5$.

We observe a statistically significant correlation between the UV slope and stellar mass. In general, galaxies with lower stellar masses tend to prefer bluer UV slopes. Given the build-up of stellar mass and dust is correlated, we expect

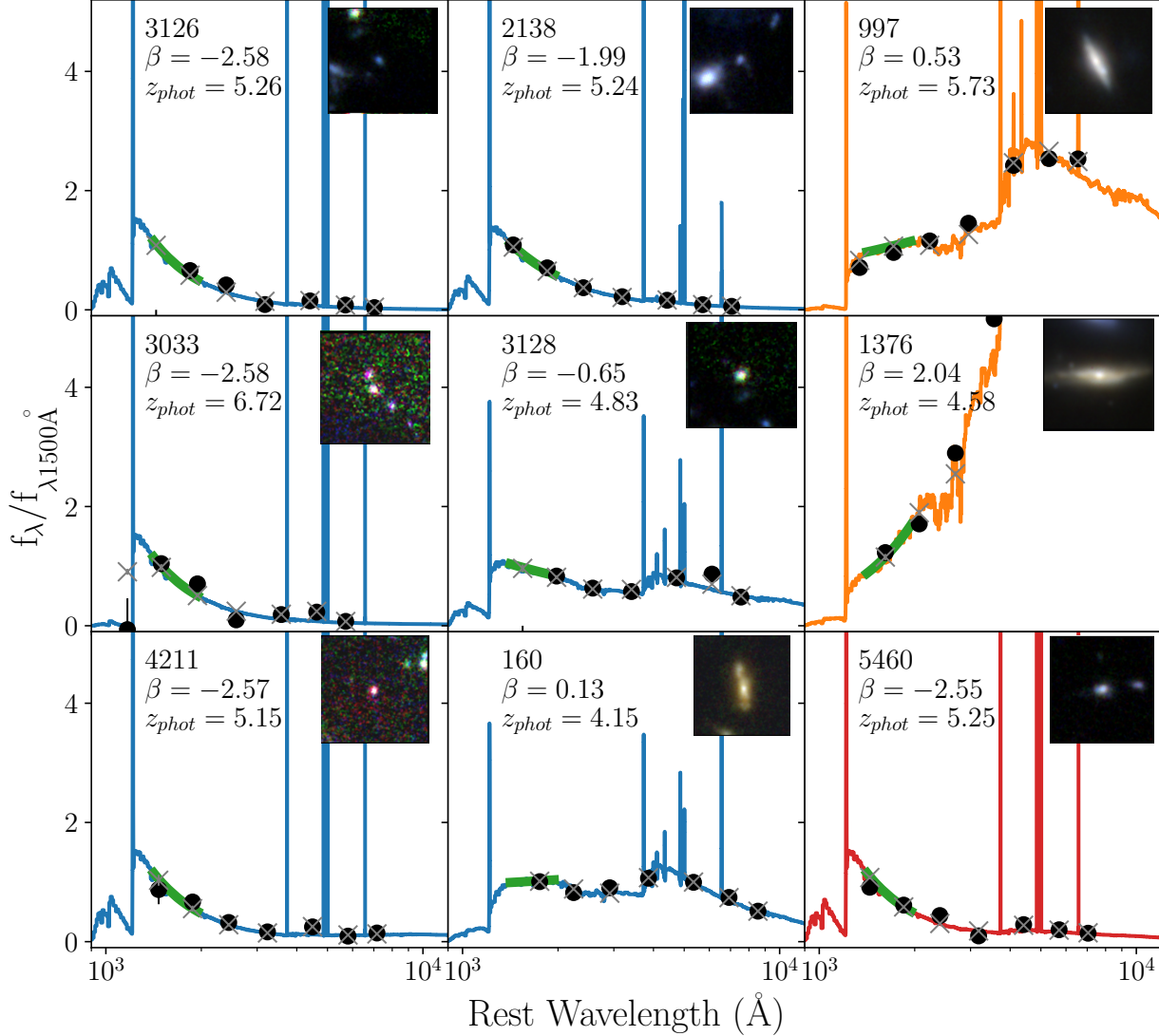


Figure 3. Here we show a representative sample of EAZY best-fit galaxy SEDs used in our analysis. Galaxies are divided into three categories based on their rest-frame UVJ color and are color coded in blue, orange, and red for blue star-forming, red/dusty star-forming, and quiescent, respectively. Best-fit EAZY SED photometry and the real observed photometry with their associated errors are shown by crosses and circles, respectively. We show the fit to the UV slope in green. The montages show rest-frame g, r, i color images of the galaxies (see *Jacobs et al. (submitted)* for details). The text in each panel gives the galaxy ID as in Paper II catalogue, the UV slope exponent, and the photometric redshift. We note that the strong emission lines in the rest- V band of $z \sim 5-6$ galaxies could lead to contamination in UVJ quiescent space.

higher stellar mass galaxies to have shallower UV slopes suggesting a higher amount of dust obscuration. Similar to the UV magnitude relationship, individual galaxies with stellar masses $\log_{10}(M_*/M_\odot) \lesssim 9$ show evidence of reaching the lower limit for UV magnitude allowed by the templates. We revisit this in Section 3.

3. THE NATURE OF THE UV SLOPES IN THE EARLY UNIVERSE

The UV slope of a galaxy is constrained by the observed photometric bands and thus can be considered as a direct ob-

servable. Traditionally, the UV slope has been a useful measurement of the dust content in galaxies where dust emission in the infra-red cannot be easily constrained (e.g. Reddy et al. 2006). At a fixed choice of an attenuation curve, the amount of reddening measures the amount of dust between the young blue O and B type stars in a galaxy and its close proximity (e.g. Calzetti et al. 1994; Meurer et al. 1999). The shallower the UV slope (i.e. more positive β values), the higher the amount of dust obscuration that is expected in galaxies. However, degeneracies between galaxy age, mass, and luminosity could add extra uncertainty in deriving the amount of dust with the UV slope (e.g. Reddy et al. 2010; Casey et al.

Table 1. Binned values for our galaxies.

Bin range	N_{sources}	Median β	σ_{β}
$4.00 < z < 4.75$	51	-2.04	0.23
$4.75 < z < 5.50$	86	-2.23	0.15
$5.50 < z < 6.25$	14	-2.03	0.09
$6.25 < z < 7.0$	27	-2.07	0.10
$-23.65 < M_{UV} < -20.28$	45	-2.09	0.14
$-20.28 < M_{UV} < -19.62$	44	-2.13	0.13
$-19.62 < M_{UV} < -19.03$	44	-2.21	0.18
$-19.03 < M_{UV} < -18.10$	45	-2.17	0.18
$8.34 < \log_{10}(M_*/M_{\odot}) < 8.79$	43	-2.62	0.13
$8.79 < \log_{10}(M_*/M_{\odot}) < 9.01$	45	-2.15	0.16
$9.01 < \log_{10}(M_*/M_{\odot}) < 9.35$	45	-2.11	0.15
$9.35 < \log_{10}(M_*/M_{\odot}) < 12.21$	45	-2.07	0.20

NOTE—Here we show the values computed for the binned samples shown by Figure 4.

2014; Bouwens et al. 2016a). While FIR detections could help alleviate this tension, the infra-red excess of galaxies at $z > 4$ is challenging to interpret due to the general reliance of a single ALMA detection to derive the total FIR luminosity. Additionally, constraining analysis to ones only with FIR detections biases analysis towards UV bright or heavily dust obscured galaxies (Hodge & da Cunha 2020).

Our analysis is purely based on a $F444W$ magnitude selected sample of galaxies where we have confident $S/N > 5$ detections in at least 4 photometric bands covering both rest-UV and optical wavelengths. Given $F444W$ band cover the rest-optical bands for our galaxies, our sample can also be reasonably assumed as a mass selected sample. We have visually inspected all multi band photometric images, SED fits, and the UV slope fits to every galaxy in the sample. Our stringent quality cuts on the EAZY best fit SEDs allow us to gain initial insights to the UV slopes of rest-optical selected galaxies at $4 < z < 7$. However, we caution that the stringent quality cuts imposed on our magnitude selected sample could lead to incompleteness and selection effects. This needs to be modeled in terms of observed photometry of the NIRCcam bands and is out of scope of this letter.

Our sample reaches UV magnitude of $M_{UV} \sim -18$, which is comparable the *Hubble* blank field data (Bouwens et al. 2022a). A modest amount of lensing magnification is expected to be present in GLASS-JWST NIRCcam parallel fields. In this initial set of papers we neglect the effect and will be revisited after the completion of the campaign. However, we stress that quantities such as the UV slope and colors are unaffected by magnification and therefore our conclusions are robust in that respect.

Bouwens et al. (2014) derived an empirical relationship between UV slope with redshift ($z \sim 4 - 7$) based on deep *HST* data reaching to $M_{UV} = -16.7$. Within our detection levels, we do not observe a clear redshift evolution of the UV slope for the GLASS-JWST data (Figure 4). However, we find that a statistically significant negative correlation exist

for galaxies with $M_{UV} < -19$. Bouwens et al. (2016b) sample is based on infrared detected Lyman-break galaxies, thus it is reasonable that these galaxies observe significantly shallower UV slopes compared to our sample. $z < 3$ galaxies (McLure et al. 2018) also show shallower UV slopes compared to our sample, specially at $\log_{10}(M_*/M_{\odot}) > 8.5$.

In Figure 4 we also show the UV slopes of the luminous Ly- α emitters observed by Jiang et al. (2020). While some of our galaxies reach $\beta \sim -2.5$, we do not reach the bluer $\beta \lesssim -3.0$ values observed in these Ly- α emitters. Jiang et al. (2020) finds that the bluer galaxies in their sample with $\beta \sim -2.7$ are challenging to be reproduced with stellar population models.

As mentioned in Section 2, our sample at lower masses and fainter UV magnitudes reach the bluer $\beta \lesssim -2.5$ limit that is capable to be fit by the a combination of empirical and theoretical SED models. This limit is evident due to the horizontal limit that is observed at the bluer UV values in the individual measurements. We further test PEGASE (Fioc & Rocca-Volmerange 2019) and FSPS (Conroy & Gunn 2010) model templates with EAZY but are unable to resolve the limitation imposed by the templates to the observed UV slopes. It is likely that a combination of Population III templates (as investigated by Bouwens et al. 2010) or models considering UV continuum leakage/AGN effects as discussed by Jiang et al. (2020) could be required to reach bluer UV slopes than what is allowed by the templates used in our analysis. As the goal of this paper series is to quickly demonstrate the capabilities of JWST data in the context of ERS, we defer a complete treatment of the analysis of UV slopes to future work.

In terms of UV magnitude, our galaxies span a large range in $M_{UV} \sim -23$ to ~ -18 . While our full sample does not show a statically significant correlation between UV magnitude and the UV slope, we find evidence for a correlation for galaxies at $z > 5$. However, we refrain from interpreting this due to selection effects that could have arisen from our bluer filters. While magnitude depths are quite constant across the bands, $F090W$ is ~ 0.2 mag shallower. Additionally, we observe a higher amount of detector defects in the bluer bands. Since galaxies with bluer UV slopes would be brighter in the bluer bands, at $4 < z < 5$ this may lead them to preferentially pass our S/N cut requirement of having $S/N > 5$ detections in minimum 4 bands.

Previous work have found conflicting results on the UV magnitude dependence on β (e.g. Finkelstein et al. 2012; Bouwens et al. 2014; Yamanaka & Yamada 2019), especially at $z > 6$. Our binned values are largely in agreement with the Bouwens et al. (2014) relation. The $z \sim 4$ LBGs in Yamanaka & Yamada (2019) sample shows redder UV slopes compared to our results. The stellar population analysis of LBGs show that they have a young star-forming stellar population with high amounts of dust. From the UVJ and ugi color analysis in Figure 2, we found that JWST-GLASS data are preferentially biased towards blue star-forming systems, as opposed to red/dusty star-forming systems. Thus, we can rule out significant dust obscuration in our galaxies, and the distinction with Yamanaka & Yamada (2019) is as expected.

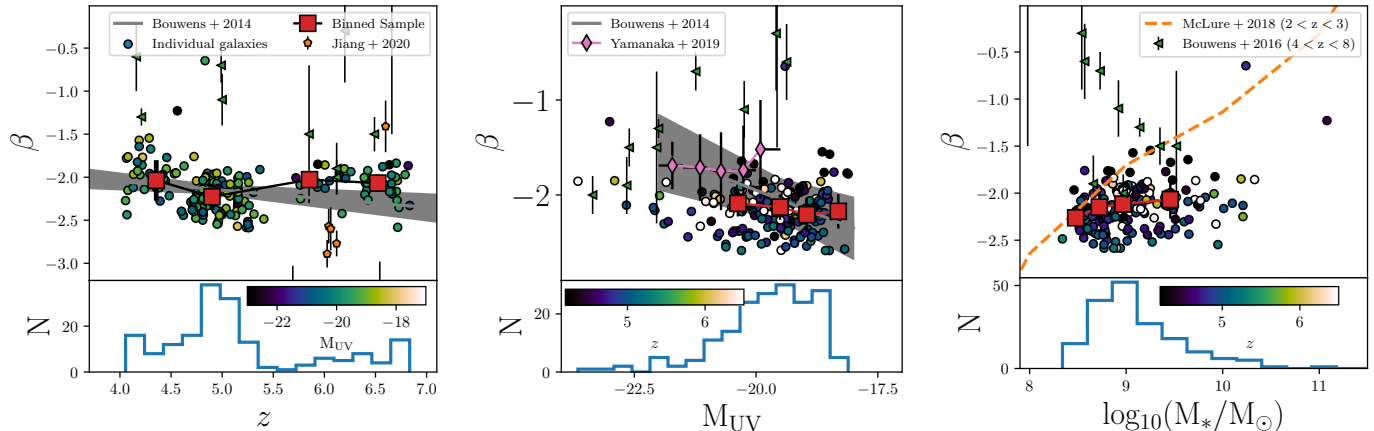


Figure 4. The relationship of the UV slope β with **Left:** redshift (colour coded in terms of UV magnitude), **Center:** rest-frame UV magnitude (colour coded in terms of redshift), and **Right:** stellar mass (colour coded in terms of redshift). Galaxies are further binned in each of the three parameters and are shown in the respective panels. Values reported by Bouwens et al. (2016b); Yamanaka & Yamada (2019); Jiang et al. (2020) as well as empirical relationships by Bouwens et al. (2014); McLure et al. (2018) are shown for comparison. We find no statically significant evolution for β with redshift, however, we find that β show a dependence on UV magnitude and stellar mass. A fraction of galaxies reach $\beta \lesssim -2.5$ suggesting that SED templates with $\beta < -2.5$ are required to accurately predict the rest-UV properties of galaxies in this epoch.

In order to determine the dust build-up in the early Universe, the UV slope evolution should be linked with stellar mass and age. As validated by the rest-frame color distributions, we expect the majority of galaxies to be blue, young star-forming systems at these redshifts. Simulations by Pop-ping et al. (2017) show that stellar age also plays a significant role in determining the UV slope. Given sources with redder UV slopes show a bias towards higher masses (Figure 4) we cannot rule out effects from age to our analysis.

Most of our galaxies have blue UV slopes. The expected median attenuation following Meurer et al. (1999) relation is $A_{v\beta} = 0.06 \pm 0.39$. Therefore, based on our GLASS-JWST NIRCcam $F444W$ selected sample, we expect galaxies at $4 < z < 7$ to be relatively dust free blue star-forming systems. Within this window the Universe was only $\sim 0.7 - 1.5$ Gyrs old, thus we expect supernovae to be the primary driver of dust buildup in these early systems (Hodge & da Cunha 2020). When compared to $z \sim 2$ K -band selected samples (e.g Shivaie et al. 2018; Nanayakkara et al. 2020), the UV slopes observed by our survey are significantly bluer. At later times, we expect AGB stars to be the dominant dust production mechanisms leading the general population of galaxies to be more dust rich.

We refrain from linking our UV slopes to expected IRX at $z > 4$. As shown by Bouwens et al. (2016b), the increase of dust temperature with redshift (B  thermin et al. 2015; Schreiber et al. 2018a) and correlations with the assumed dust attenuation curve could add biases to the UV slope-IRX relationship. If galaxies at early times show harder ionizing spectra with high-energy emission lines (e.g Mainali et al. 2018; Nanayakkara et al. 2019), the relationship between dust production and relationship becomes important. Furthermore, any evolution of the IMF with redshift (Nanayakkara et al. 2017; Sneppen et al. 2022) would add

further complications to interpreting the UV slope-dust evolution with redshift.

4. CONCLUSIONS AND FUTURE WORK

We have presented a first view from JWST on the UV slope evolution of NIRCcam $F444W$ selected galaxies at $z \sim 4 - 7$ from our GLASS-JWST program.

- We find that a majority of our galaxies ($> 95\%$) are blue star-forming systems with steep UV slopes.
- We find a statistically significant evolution of the UV slopes with redshift for $M_{UV} < -20$ galaxies, but not for the full GLASS-JWST sample which span $M_{UV} \sim -23.6$ to -18.1 .
- We find that galaxies with faint UV magnitudes and low stellar masses have bluer UV slopes compared to their UV bright high mass counterparts. This suggest that faint UV systems observed by JWST are blue, low SFR systems.
- We find that individual measurements of UV slopes hit the bluer limits imposed by the SED templates used in our analysis.

In the context of empirical and theoretical SED models based on stellar population synthesis models such as FSPS and PEGASE, we are unable to obtain bluer UV slopes than what is presented in our analysis. Therefore, we expect that a detailed treatment with models that include Population III dust free stars (e.g Bouwens et al. 2010) or other effects that are not considered in the current SED models are required to accurately predict the UV slopes/properties of galaxies which will be routinely observed in the early Universe with JWST.

Here we have found that rest-optical selected galaxies at $4 < z < 7$ are preferentially blue star-forming galaxies with

steep UV slopes. Future work should focus on sample selection effects to determine the real number density of extreme blue systems in the early Universe. By combining deep NIR-Cam observations between different ERS and JWST Cycle 1 treasury programs, a large representative sample of galaxies at these redshifts could be constructed to analyze the evolution of the UV slope with redshift and UV magnitude. Obtaining constraints to the infrared emission and dust temperatures using deep JWST/MIRI and ALMA observations (Schreiber et al. 2018a) planned on JWST ERS/Treasury fields and ISM conditions from JWST/NIRSpec observations would add important diagnostic power to determine how the evolution of mass and dust was modulated in the early Universe.

Facility: JWST: (NIRCam)

This work is based on observations made with the NASA/ESA/CSA James Webb Space Telescope. The data were obtained from the Mikulski Archive for Space Telescopes at the Space Telescope Science Institute, which is operated by the Association of Universities for Research in Astronomy, Inc., under NASA contract NAS 5-03127 for JWST. These observations are associated with program JWST-ERS-1342. We acknowledge financial support from NASA through grant JWST-ERS-1324. T.N., K. G., and C.J. acknowledge support from Australian Research Council Laureate Fellowship FL180100060. MB acknowledges support from the Slovenian national research agency ARRS through grant N1-0238. CM acknowledges support by the VILLUM FONDEN under grant 37459. The Cosmic Dawn Center (DAWN) is funded by the Danish National Research Foundation under grant DNRF140. This project made use of *astropy* (Astropy Collaboration et al. 2018), *matplotlib* (Hunter 2007), and *pandas* (pandas development team 2020).

REFERENCES

- Antwi-Danso, J., Papovich, C., Leja, J., et al. 2022, arXiv e-prints, arXiv:2207.07170. <https://arxiv.org/abs/2207.07170>
- Astropy Collaboration, Price-Whelan, A. M., Sipőcz, B. M., et al. 2018, *AJ*, 156, 123, doi: [10.3847/1538-3881/aabc4f](https://doi.org/10.3847/1538-3881/aabc4f)
- Béthermin, M., Daddi, E., Magdis, G., et al. 2015, *A&A*, 573, A113, doi: [10.1051/0004-6361/201425031](https://doi.org/10.1051/0004-6361/201425031)
- Bouwens, R. J., Illingworth, G., Ellis, R. S., et al. 2022a, *ApJ*, 931, 81, doi: [10.3847/1538-4357/ac618c](https://doi.org/10.3847/1538-4357/ac618c)
- Bouwens, R. J., Illingworth, G. D., Ellis, R. S., Oesch, P. A., & Stefanon, M. 2022b, arXiv e-prints, arXiv:2205.11526. <https://arxiv.org/abs/2205.11526>
- Bouwens, R. J., Smit, R., Labbé, I., et al. 2016a, *ApJ*, 831, 176, doi: [10.3847/0004-637X/831/2/176](https://doi.org/10.3847/0004-637X/831/2/176)
- Bouwens, R. J., Illingworth, G. D., Oesch, P. A., et al. 2010, *ApJL*, 708, L69, doi: [10.1088/2041-8205/708/2/L69](https://doi.org/10.1088/2041-8205/708/2/L69)
- . 2014, *ApJ*, 793, 115, doi: [10.1088/0004-637X/793/2/115](https://doi.org/10.1088/0004-637X/793/2/115)
- Bouwens, R. J., Aravena, M., Decarli, R., et al. 2016b, *ApJ*, 833, 72, doi: [10.3847/1538-4357/833/1/72](https://doi.org/10.3847/1538-4357/833/1/72)
- Bouwens, R. J., Oesch, P. A., Stefanon, M., et al. 2021, *AJ*, 162, 47, doi: [10.3847/1538-3881/abf83e](https://doi.org/10.3847/1538-3881/abf83e)
- Bouwens, R. J., Smit, R., Schouws, S., et al. 2022c, *ApJ*, 931, 160, doi: [10.3847/1538-4357/ac5a4a](https://doi.org/10.3847/1538-4357/ac5a4a)
- Bradač, M. 2020, *Nature Astronomy*, 4, 478, doi: [10.1038/s41550-020-1104-5](https://doi.org/10.1038/s41550-020-1104-5)
- Brammer, G. B., van Dokkum, P. G., & Coppi, P. 2008, *ApJ*, 686, 1503, doi: [10.1086/591786](https://doi.org/10.1086/591786)
- Bromm, V., & Yoshida, N. 2011, *ARA&A*, 49, 373, doi: [10.1146/annurev-astro-081710-102608](https://doi.org/10.1146/annurev-astro-081710-102608)
- Bruzual, G., & Charlot, S. 2003, *MNRAS*, 344, 1000, doi: [10.1046/j.1365-8711.2003.06897.x](https://doi.org/10.1046/j.1365-8711.2003.06897.x)

- Burriesci, L. G. 2005, in Society of Photo-Optical Instrumentation Engineers (SPIE) Conference Series, Vol. 5904, Cryogenic Optical Systems and Instruments XI, ed. J. B. Heaney & L. G. Burriesci, 21–29, doi: [10.1117/12.613596](https://doi.org/10.1117/12.613596)
- Calzetti, D., Armus, L., Bohlin, R. C., et al. 2000, *ApJ*, 533, 682, doi: [10.1086/308692](https://doi.org/10.1086/308692)
- Calzetti, D., Kinney, A. L., & Storchi-Bergmann, T. 1994, *ApJ*, 429, 582, doi: [10.1086/174346](https://doi.org/10.1086/174346)
- Casey, C. M., Scoville, N. Z., Sanders, D. B., et al. 2014, *ApJ*, 796, 95, doi: [10.1088/0004-637X/796/2/95](https://doi.org/10.1088/0004-637X/796/2/95)
- Chabrier, G. 2003, *Publications of the Astronomical Society of the Pacific*, 115, pp. 763.
<http://www.jstor.org/stable/10.1086/376392>
- Conroy, C., & Gunn, J. E. 2010, *ApJ*, 712, 833, doi: [10.1088/0004-637X/712/2/833](https://doi.org/10.1088/0004-637X/712/2/833)
- Dayal, P., & Ferrara, A. 2018, *PhR*, 780, 1, doi: [10.1016/j.physrep.2018.10.002](https://doi.org/10.1016/j.physrep.2018.10.002)
- Dayal, P., Ferrara, A., Sommovigo, L., et al. 2022, *MNRAS*, 512, 989, doi: [10.1093/mnras/stac537](https://doi.org/10.1093/mnras/stac537)
- Endsley, R., & Stark, D. P. 2022, *MNRAS*, 511, 6042, doi: [10.1093/mnras/stac524](https://doi.org/10.1093/mnras/stac524)
- Finkelstein, S. L., Papovich, C., Salmon, B., et al. 2012, *ApJ*, 756, 164, doi: [10.1088/0004-637X/756/2/164](https://doi.org/10.1088/0004-637X/756/2/164)
- Finkelstein, S. L., Bagley, M., Song, M., et al. 2022, *ApJ*, 928, 52, doi: [10.3847/1538-4357/ac3aed](https://doi.org/10.3847/1538-4357/ac3aed)
- Fioc, M., & Rocca-Volmerange, B. 2019, arXiv e-prints, arXiv:1902.02198. <https://arxiv.org/abs/1902.02198>
- Hashimoto, T., Inoue, A. K., Mawatari, K., et al. 2018, ArXiv e-prints. <https://arxiv.org/abs/1806.00486>
- Hodge, J. A., & da Cunha, E. 2020, *Royal Society Open Science*, 7, 200556, doi: [10.1098/rsos.200556](https://doi.org/10.1098/rsos.200556)
- Hunter, J. D. 2007, *Computing In Science & Engineering*, 9, 90
- Jiang, L., Cohen, S. H., Windhorst, R. A., et al. 2020, *ApJ*, 889, 90, doi: [10.3847/1538-4357/ab64ea](https://doi.org/10.3847/1538-4357/ab64ea)
- Jung, I., Finkelstein, S. L., Dickinson, M., et al. 2019, *ApJ*, 877, 146, doi: [10.3847/1538-4357/ab1bde](https://doi.org/10.3847/1538-4357/ab1bde)
- Le Reste, A., Hayes, M., Cannon, J. M., et al. 2022, arXiv e-prints, arXiv:2206.06374. <https://arxiv.org/abs/2206.06374>
- Leethochawalit, N., Roberts-Borsani, G., Morishita, T., Trenti, M., & Treu, T. 2022, arXiv e-prints, arXiv:2205.15388. <https://arxiv.org/abs/2205.15388>
- Leonova, E., Oesch, P. A., Qin, Y., et al. 2021, arXiv e-prints, arXiv:2112.07675. <https://arxiv.org/abs/2112.07675>
- Madau, P., & Dickinson, M. 2014, *ARA&A*, 52, 415, doi: [10.1146/annurev-astro-081811-125615](https://doi.org/10.1146/annurev-astro-081811-125615)
- Mainali, R., Zitrin, A., Stark, D. P., et al. 2018, *MNRAS*, 479, 1180, doi: [10.1093/mnras/sty1640](https://doi.org/10.1093/mnras/sty1640)
- Matthee, J., Sobral, D., Gronke, M., et al. 2018, ArXiv e-prints, arXiv:1805.11621. <https://arxiv.org/abs/1805.11621>
- McLure, R. J., Pentericci, L., Cimatti, A., et al. 2018, *MNRAS*, 479, 25, doi: [10.1093/mnras/sty1213](https://doi.org/10.1093/mnras/sty1213)
- Merlin, E., Fortuni, F., Torelli, M., et al. 2019, *MNRAS*, 490, 3309, doi: [10.1093/mnras/stz2615](https://doi.org/10.1093/mnras/stz2615)
- Meurer, G. R., Heckman, T. M., & Calzetti, D. 1999, *ApJ*, 521, 64, doi: [10.1086/307523](https://doi.org/10.1086/307523)
- Naidu, R. P., Tacchella, S., Mason, C. A., et al. 2019, arXiv e-prints, arXiv:1907.13130. <https://arxiv.org/abs/1907.13130>
- Nanayakkara, T., Glazebrook, K., Kacprzak, G. G., et al. 2017, *MNRAS*, 468, 3071, doi: [10.1093/mnras/stx605](https://doi.org/10.1093/mnras/stx605)
- Nanayakkara, T., Brinchmann, J., Boogaard, L., et al. 2019, *A&A*, 624, A89, doi: [10.1051/0004-6361/201834565](https://doi.org/10.1051/0004-6361/201834565)
- Nanayakkara, T., Brinchmann, J., Glazebrook, K., et al. 2020, *ApJ*, 889, 180, doi: [10.3847/1538-4357/ab65eb](https://doi.org/10.3847/1538-4357/ab65eb)
- Newville, M., Stensitzki, T., Allen, D. B., & Ingargiola, A. 2014, LMFIT: Non-Linear Least-Square Minimization and Curve-Fitting for Python, 0.8.0, Zenodo, Zenodo, doi: [10.5281/zenodo.11813](https://doi.org/10.5281/zenodo.11813)
- Oesch, P. A., van Dokkum, P. G., Illingworth, G. D., et al. 2015, *ApJ*, 804, L30, doi: [10.1088/2041-8205/804/2/L30](https://doi.org/10.1088/2041-8205/804/2/L30)
- Oke, J. B., & Gunn, J. E. 1983, *ApJ*, 266, 713, doi: [10.1086/160817](https://doi.org/10.1086/160817)
- pandas development team, T. 2020, pandas-dev/pandas: Pandas, latest, Zenodo, doi: [10.5281/zenodo.3509134](https://doi.org/10.5281/zenodo.3509134)
- Popping, G., Puglisi, A., & Norman, C. A. 2017, *MNRAS*, 472, 2315, doi: [10.1093/mnras/stx2202](https://doi.org/10.1093/mnras/stx2202)
- Reddy, N. A., Erb, D. K., Pettini, M., Steidel, C. C., & Shapley, A. E. 2010, *ApJ*, 712, 1070, doi: [10.1088/0004-637X/712/2/1070](https://doi.org/10.1088/0004-637X/712/2/1070)
- Reddy, N. A., Steidel, C. C., Fadda, D., et al. 2006, *ApJ*, 644, 792, doi: [10.1086/503739](https://doi.org/10.1086/503739)
- Reddy, N. A., Oesch, P. A., Bouwens, R. J., et al. 2018, *ApJ*, 853, 56, doi: [10.3847/1538-4357/aaa3e7](https://doi.org/10.3847/1538-4357/aaa3e7)
- Roberts-Borsani, G., Morishita, T., Treu, T., Leethochawalit, N., & Trenti, M. 2022, *ApJ*, 927, 236, doi: [10.3847/1538-4357/ac4803](https://doi.org/10.3847/1538-4357/ac4803)
- Schreiber, C., Elbaz, D., Pannella, M., et al. 2018a, *A&A*, 609, A30, doi: [10.1051/0004-6361/201731506](https://doi.org/10.1051/0004-6361/201731506)
- Schreiber, C., Glazebrook, K., Nanayakkara, T., et al. 2018b, *A&A*, 618, A85, doi: [10.1051/0004-6361/201833070](https://doi.org/10.1051/0004-6361/201833070)
- Shivaei, I., Reddy, N. A., Siana, B., et al. 2018, *ApJ*, 855, 42, doi: [10.3847/1538-4357/aaad62](https://doi.org/10.3847/1538-4357/aaad62)
- Sneppen, A., Steinhardt, C. L., Hensley, H., et al. 2022, *ApJ*, 931, 57, doi: [10.3847/1538-4357/ac695e](https://doi.org/10.3847/1538-4357/ac695e)
- Spearman, C. 1904, *The American Journal of Psychology*, 15, 72. <http://www.jstor.org/stable/1412159>
- Spitler, L. R., Straatman, C. M. S., Labbé, I., et al. 2014, *ApJL*, 787, L36, doi: [10.1088/2041-8205/787/2/L36](https://doi.org/10.1088/2041-8205/787/2/L36)
- Stark, D. P. 2016, *ARA&A*, 54, 761, doi: [10.1146/annurev-astro-081915-023417](https://doi.org/10.1146/annurev-astro-081915-023417)
- Stefanon, M., Bouwens, R. J., Labbé, I., et al. 2022, *ApJ*, 927, 48, doi: [10.3847/1538-4357/ac3de7](https://doi.org/10.3847/1538-4357/ac3de7)

- Stefanon, M., Labbé, I., Oesch, P. A., et al. 2021, *ApJS*, 257, 68, doi: [10.3847/1538-4365/ac2498](https://doi.org/10.3847/1538-4365/ac2498)
- Strait, V., Bradač, M., Coe, D., et al. 2021, *ApJ*, 910, 135, doi: [10.3847/1538-4357/abe533](https://doi.org/10.3847/1538-4357/abe533)
- Tacchella, S., Finkelstein, S. L., Bagley, M., et al. 2022, *ApJ*, 927, 170, doi: [10.3847/1538-4357/ac4cad](https://doi.org/10.3847/1538-4357/ac4cad)
- Treu, T., Roberts-Borsani, G., Bradac, M., et al. 2022, *ApJ*, in press, arXiv:2206.07978. <https://arxiv.org/abs/2206.07978>
- Wilkins, S. M., Bouwens, R. J., Oesch, P. A., et al. 2016, *MNRAS*, 455, 659, doi: [10.1093/mnras/stv2263](https://doi.org/10.1093/mnras/stv2263)
- Williams, R. J., Quadri, R. F., Franx, M., van Dokkum, P., & Labbé, I. 2009, *ApJ*, 691, 1879, doi: [10.1088/0004-637X/691/2/1879](https://doi.org/10.1088/0004-637X/691/2/1879)
- Yamanaka, S., & Yamada, T. 2019, *PASJ*, 71, 51, doi: [10.1093/pasj/psz024](https://doi.org/10.1093/pasj/psz024)
- Yang, L., Leethochawalit, N., Treu, T., et al. 2022, *MNRAS*, 514, 1148, doi: [10.1093/mnras/stac1236](https://doi.org/10.1093/mnras/stac1236)